Accepted Manuscript

The impact of latent heat exchanges on the design of Earth Air Heat Exchangers

Emanuel Estrada[1], Matthieu Labat[2], Sylvie Lorente[2], Luiz A.O. Rocha[3]

[1] PROMEC, Universidade Federal do Rio Grande, Brazil

[2] LMDC, INSA/UPS Génie Civil, 135 Avenue de Rangueil, 31077 Toulouse cedex 04 France.

[3] Mechanical Engineering Graduate Program, Universidade do Vale do Rio dos Sinos, 93022-000 São Leopoldo, Rio Grande do Sul, Brazil.

Abstract:

The work documents the design of Earth-Air Heat Exchangers based not only on sensible heat transfer, but also on latent heat exchanges. We compare the impact of the climate of Brazil and south of France on the relevance of such systems. The duct length is determined in order to obtain maximum underground heat exchanges. A time dependent model combined to actual weather data is developed to show when an underground heat exchanger becomes a good option in a tropical climate. The three-dimensional version of the model accounts for heat transfer in the soil and for heat and moisture transfer along the underground pipe. The comparison with a 1D model allows to propose a straightforward approach to assess the cooling/heating potential of different climatic regions.

Nomenclature:

Latin Symbols	Description	Unit
A	Cross section	m^2

c_p	Specific heat	$J \cdot kg^{-1} \cdot K^{-1}$
D	Inner diameter	m
D_v	Mass diffusivity	$m^2 \cdot s^{-1}$
f	Friction factor	$m^2 \cdot s^{-1}$
h	Specific enthalpy	$kJ \cdot kg^{-1}$
h_c	Convective heat transfer coefficient	$W \cdot K^{-1} \cdot m^{-2}$
h_m	Convective mass transfer coefficient	$kg \cdot m^{-2} \cdot s^{-1}$
k	Thermal conductivity	$W \cdot m^{-1} \cdot K^{-1}$
L	Length	m
Le	Lewis Number	-
L_v	Latent heat	$kJ \cdot kg^{-1}$
$\dot{}$	Mass flow rate	$kg \cdot s^{-1}$
Nu	Nusselt number	-
p	Perimeter	m
P	Pressure	Pa
P'	Period	hour
Pr	Prandtl number	-
$\dot{q}$	Heat transfer rate	W
Re_D	Reynolds number	-
Sh	Sherwood Number	-
t	time	s
T	Temperature	°C
w	Moisture content	kg_{vapor}/kg_{air}

Greek Symbols

α	Thermal diffusivity	$m^2 \cdot s^{-1}$

γ	Inverse of the damping depth	m^{-1}
δ	Temperature difference	K
η	Coefficient (Eq. 5)	-
ρ	Density	$kg \cdot m^{-3}$
φ	Relative humidity	-

Subscripts

a	Air
ha	Humid air
in	Inlet
sat	Saturation
v	Vapor
w	Wall

1. Introduction and background

An earth-air heat exchanger (EAHE) consists of one or several ducts buried in the ground, connected from one end to the outdoor air, and to the other end to the ventilation system of a building. Because of the high thermal inertia of the soil, the outdoor temperature variations are progressively smoothed along with the soil depth. Therefore, the ground can be considered as a huge thermal reservoir, which temperature remains milder and more stable than the outdoor air temperature all over the year. The air temperature at the pipe outlet is different from the inlet thanks to the heat exchanges occurring with the soil. This potentially allows reducing the heating or cooling loads at building scale.

Most cases are related to office buildings or typical residential buildings. A considerable number of papers focused on greenhouses [1–6], yet heat and mass loads differ strongly from buildings. At the

design stage, the impact of the pipes length, the number of pipes, the cross section of the pipe and the pipe depth have to be determined in order to enhance the EAHE performances. The latter is of significance. Most authors advise burying the pipes as deeply as possible in order to take advantage on the ground thermal inertia. The excavation cost is the sole feature limiting the pipe depth, which generally remains between 1 and 3 meters. As observed in [7], a deeply buried pipe should indeed be effective at smoothing yearly temperature variations. However, it may be worth smoothing daily variations instead, depending on the building loads and on the local climate. This could be easily achieved by burying pipes less deeply.

Many authors rely on heat transfer calculations to give a comprehensive analysis of the thermal behavior of EAHE and to improve its design. The methodology differs in terms of complexity and computational time. For example, the transient heat transfer taking place in the pipe was solved analytically in [8] under strong assumptions such as undisturbed soil surface temperature. Such an approach allows to integrate easily the EAHE model in a building simulation tool, as exemplified in [9,10]. Heat transfer in the ground was modelled to obtain more realistic results, as in [4,11-13]. A more refined approach was presented in [11], where a Computational Fluid Dynamic code was used to model the air transfer in the pipes whereas heat transfer in the ground was modelled up to a depth of 15m. However because of the high computational time, some simplifications were needed, like by considering a smaller domain for heat transfer in the soil. A possible alternative is to use model reduction techniques as presented in [14] in the case of borehole heat exchangers. The drawback of these techniques is that they are time-consuming and should not be employed for feasibility studies.

The work presented in this paper takes place in the framework of a larger project which intends to define the potential of EAHE in Brazil. Many EAHE were built over the world during the last decades, which resulted in a wide range of systems installed under different climates: 18 examples were reviewed in Santamouris et al. [1], examples of the Mediterranean climate can be found in [1–4,9], while the central European climate is considered in [7,8,15-17] and finally hot climates are

studied in [11,18,19] (humid), and in [10,20] (dry). Most systems were designed under rather dry climatic conditions, and humid climates, such as in Brazil, were not studied as intensively. Still, 8 Brazilian climates were compared in [19] and the potential benefits of EAHA were discussed. In the state of Rio Grande Do Sul, Vaz et al. [18] indicated that the air temperature change from the pipe entrance to its exit was on an average of 2K. Unlike under a continental climate where the soil temperature can be, at an equivalent depth, up to 10K lower than the ambient temperature because of seasonal time-lag, the Brazilian climate does not allow such temperature amplitudes. As a result, the relevance of EAHE systems is not very clear under Brazilian climatic conditions. One of this study objectives is to give insight on this issue.

A key feature is that the temperature decrease is not the sole impact of an EAHE in cooling mode; the system may also influence the air moisture content, and as a consequence the indoor moisture balance. The indoor relative humidity tends to increase during the night and to decrease during daytime when using an EAHE. High indoor relative humidity is not desirable as it negatively impacts indoor air quality [21], enhances fungal and mold growth [3] and may lead to sanitary problems [7]. Regarding energy savings however, the EAHE efficiency can be increased by 25% by mass transfer in summer conditions, and decreased by 20% in winter conditions in central Europe (Switzerland), as underlined in [8]. We considered that the influence of moisture transfer on the global performances of an EAHE is sizeable and worth investigating for the specific case of Brazilian climates.

As underlined in [4,8,22], moisture transfer occurs along the pipe and may significantly influence the efficiency of the heat exchanger. Condensation may happen if the dew temperature of air at the inlet is higher than the surface temperature of the pipe. From a technical viewpoint, it means that the pipe network should be embedded with a slight slope in order to drive the condensed water to a location where it could be collected and pumped outside the network. This aspect is hardly accounted for in the modelling or discussed in the result analysis. In a monitored greenhouse equipped with an EAHE [3,4], the authors estimated that the latent heat transfer (coming from condensation and/or

5

evaporation) represented 30% of the global energy balance. A similar ratio was computed in [8], yet the authors indicated that the latent part of heat transfer was mostly dominated by water infiltrations in the pipes, rather than condensation or evaporation. The analysis of the numerical results shows that sensible heat transfer is predominant on the first 10 meters in the pipe, and that latent heat transfer becomes dominant further.

In this work, we study the energetic potential of an EAHE not only based on sensible heat exchanges but also on latent heat exchanges. We consider a building where a refrigerating unit is used to permanently maintain comfortable indoor conditions. The EAHE is used in complement. More precisely, we intend to find the conditions for which an EAHE system meets the objectives of reducing the air conditioning needs under a climate such as the one of Brazil. Usually, cooling is synonymous with decreasing the temperature between the inlet and the outlet of the pipe. As the basic feature of an EAHE is to pre-cool the air blown into the house in summer, a decrease in the energy consumption of the refrigeration system is expected. However, moisture condensation happens almost systematically within a refrigerating unit and accounts for a large part of its energy consumption. Using an EAHE may not systematically yield to lower the energy consumption of the refrigerating unit, because of possible moisture increase through the pipe. The refrigerating unit must remove the excess moisture which increases the overall cooling load. This can be simply illustrated by considering the psychrometric diagram (Fig 1), which includes both the sensible and the latent heat through the enthalpy of humid air. Let us assume that the temperature and relative humidity air at the inlet of the pipe are T_{in} and RH_{in} respectively. The dew point temperature is denoted by T_{dew}, and the humid temperature is denoted by T_{humid}. If T_w is the temperature of the pipe wall and assuming a perfect heat exchanger, one can distinguish 3 different configurations, represented by 3 areas in Fig 1:

- Configuration A ($T_w < T_{dew}$): the moisture content at the outlet is lower than at the inlet, which further reduces the cooling load.

6

- Configuration B ($T_{dew} < T_w < T_{humid}$): the moisture content increased, but the enthalpy of humid air is reduced, so the cooling load is still diminished.

- Configuration C ($T_{humid} < T_w < T_{in}$): the moisture content increased in such a way that the enthalpy is higher at the outlet, yet the temperature has decreased. Obviously, the EAHE should not be used in this case.

These cases would be obtained if the wall was completely wet and the pipe was long enough. More probably, the properties of humid air at the outlet will range between the ones at the inlet (h_{in}) and the pipe wall (h_w). In sum, an EAHE will effectively reduce the cooling loads of a refrigerating unit as soon as the wall temperature remains below the humid temperature of outdoor air. If the latter is exceeded, the presence of water inside the pipe will increase the enthalpy, which will make the EAHE inefficient. Yet latent heat is hardly considered in the design of EAHE.

This paper investigates how an EAHE would perform in a humid climate, and if its use would effectively lead to energy savings. As Brazil is a country with a wide range of climates, the work is not limited to one single location. For comparison purposes, the weather conditions of a European country where it is acknowledged that EAHE systems perform well is also considered. The study starts with a simplified approach applied to a rather wide range of Brazilian climate, then the complexity of the physics is progressively increased while focusing on the regional Brazilian climates which seem the most promising for an EAHE implementation. The paper is divided as follows: the next section is dedicated to the definition of the cooling potential of EAHE, based on simple indicators which can be obtained from general climatic conditions. An analytical model of EAHE accounting for heat and mass transfer within the pipe in steady state is presented in section 3. The latter is used to highlight the influence of latent heat transfer in the global EAHE energy performances and to set the length of the pipe. Next steps consist in the time-dependent modelling of heat transfer in the pipe, while the heat transfer in the soil is finally included in the last section.

2. Cooling potential

2.1 Thermal characteristics in the French and Brazilian locations

We consider two different countries (Fig. 2): One is Brazil, while the other is France and more specifically the region of Montpellier. Such locations correspond to the choice of places with relatively hot temperatures in the summer and different moisture levels. For example, the annual mean temperature and relative humidity are 23.15°C and 78.3% in Rio do Janeiro, and 14.82°C and 68.7% in Montpellier, while the annual temperature amplitude is 2.73 K for Rio do Janeiro, and 12.1 K for Montpellier.

The soil temperature is obtained from the analytical function [23]:

$$T(z, t) = T_m + A_z \, sin \left[\frac{2\pi \, (t - t_0)}{P'} - \gamma \, z - \frac{\pi}{2} \right] \tag{1}$$

where $T(z, t)$ is the soil temperature at time t and depth z, T_m is mean temperature at the soil surface and t_0 is the time lag needed for the soil surface temperature to reach T_m. In Eq. (1) A_z is the amplitude of the temperature wave at a depth z, and time t, and decays exponentially with the depth as follows:

$$A_z = A_0 exp \, (-\gamma \, z) \tag{2}$$

The inverse of the damping depth, γ, is

$$\gamma = \sqrt{\frac{\pi}{\alpha P'}} \tag{3}$$

where P' is the period of the oscillation (1 year here, expressed in hours) and α is the soil thermal diffusivity which is considered constant. Equation (1) assumes also that the heat flux is one-

8

dimensional and the surface temperature $T(0,t)$ equals the air temperature [24]. The parameters T_m, and A_0 were extracted from weather data provided by the internet databases Energy Plus [25] and INMET [26]. $T(0,t)$ is obtained by curve fitting the weather data to get the parameters A_0 and t_0. Table 1 shows the values used for each region. The soil thermal diffusivity was chosen identical in all the cases ($\alpha = 0.0023$ m^2/h in Eq. (3)).

Table 1: Soil function parameters

City	Belem	Brasilia	Curitiba	Porto Alegre	Recife	Rio do Janeiro	Santa Maria	Sao Paulo	Montpellier (France)
T_m (°C)	26.47	21.28	17.17	20.03	25.75	23.15	19.04	19.57	14.82
A_0 (°C)	0.62	1.65	4.08	5.00	1.51	2.73	5.11	2.33	12.10
t_0 (h)	1917	4153	4901	4798	4824	4941	4861	4801	648

Figure 3 shows the envelope of the extreme temperatures reached by the soil over the year for Rio do Janeiro and Montpellier. See the large temperature amplitude of the soil temperature in the South of France relatively to the values measured in Rio.

2.2 First estimation of the potential of EAHE

To give a first estimation of the potential of EAHE for reducing the cooling loads of a refrigerating unit, we propose to rely on the assumption developed in the introduction: the use of an EAHE is beneficial if the temperature of the wall of the buried pipe (T_w) is lower than the humid temperature of outdoor air (T_{humid}). The latter was computed based on hourly climatic data (relative humidity and dry bulb temperature). We considered that the pipe was buried at a depth of about 3 meters following [27]. The pipe wall temperature T_w is assumed to be the soil temperature at the considered depth, and is calculated based on Eq. (1). Assume δ is the temperature difference between T_{humid} and the wall.

9

$$\delta = T_{humid} - T_w \tag{4}$$

A positive value means that the EAHE would help reducing the cooling load. η represents the time (in %) in the month during which using the EAHE is beneficial.

$$\eta = \frac{t_{\delta>0}}{t_{\delta>0} + t_{\delta<0}} \tag{5}$$

Figure 4 allows to identify two different behaviors. η is lower than 5% all over the year in the regions of Belem, Brasilia and Recife. Higher values of η were obtained for Curitiba, Rio, Porto Alegre, Santa Maria and Sao Paulo (up to 79% for Curitiba in January). Given the criterion proposed here (based on the humid temperature), it seems relevant to use an EAHE for these 5 locations, yet for a limited period of time only. This result can be linked to the A_0 parameter (see Table 1) which represents the amplitude of the temperature variation over one year at the soil surface: the lowest values of η were obtained for locations with the lowest A_0, meaning that the potential of the EAHE for cooling decreases along with seasonal temperature amplitude. This approach does not give any information on the energy savings potential. Yet, it clearly exhibits the differences between the different Brazilian climates. Considering Fig.1 and Fig. 4, the EAHE energy savings potential is greater in the southern part of the country.

3. Steady state analysis

This section details the heat and mass transfer model developed within the pipe. First, the steady-state heat and mass balances are presented. This approach allows to determine one of the EAHE design parameters: the pipe length above which no significant improvement would be observed.

3.1 Analytical model

A conceptual sketch of the earth air heat exchanger (EAHE) is shown in Fig. 5. The system consists of a fan blowing air into a cylindrical duct. The exact position of the fan does not matter, as long as the electrical motor is located outside the duct. Otherwise, the heat dissipated by the engine should

be accounted for in the energy balance, and may influence the thermal efficiency of the heat exchanger. For the sake of simplicity, the geometry of the system at the inlet and at the outlet was not considered in this study; the region of interest is the horizontal part of EAHE of length L and diameter D.

Consider the elemental volume of thickness dx represented in Fig. 5. We assume that the entire pipe surface is wet because of water infiltration. For more details on this assumption, see [28]. This is an extreme case, the opposite case (dry wall) will be considered later. The wall temperature is T_w. Air enters the pipe at T_{in} and RH_{in}, with $T_{in} > T_w$. If T_w is below the dew point temperature, because the moisture content of the air at inlet is higher than the wall moisture content, the vapor carried by the air flow along the duct will condensate.

The mass flow rate of humid air is written $\dot{m}_{ha}$, and $\dot{m}_{ha} = \dot{m}_a + \dot{m}_v$ where $\dot{m}_a$ is the dry air mass flow rate and $\dot{m}_v$ is the vapor mass flow rate.

Mass conservation requires

$$d\dot{m}_{v,x} = d\dot{m}_{v,x+dx} + d\dot{m}_{cond,dx} \tag{6}$$

where $d\dot{m}_{cond,dx}$ represents the condensed water in time along dx.

The energy conservation in steady state writes

$$(\dot{m}\,h)_{ha,x} = d\dot{q} + (\dot{m}\,h)_{ha,x+dx} \tag{7}$$

where h is the specific enthalpy.

Equation (7) can be written as

$$d\dot{q} = -d(\dot{m}_a\,h_{ha}) \tag{8}$$

11

The specific enthalpy of humid air is $h_{ha} = c_{P,a} T + w(c_{P,v} T + L_v)$, where $c_{P,a}$ and $c_{P,v}$ are respectively the heat capacity of air and vapor, w is the water content, and L_v is the latent heat of evaporation/condensation.

The heat transfer rate has two contributions. The first one is due to sensible heat transfer, while the second contribution appears because of condensation: $d\dot{m}_{cond} \times L_v$. The mass flow rate of condensed water $d\dot{m}_{cond}$ in the elemental domain is given by

$$d\dot{m}_{cond} = h_m \, p \, dx \, \rho_{ha}[w - w_w] \tag{9}$$

where p is the duct perimeter, h_m is the mass transfer coefficient, ρ_{ha} is the humid air density. We have

$$d\dot{q} = h_c \, p \, dx(T - T_w) + h_m \, p \, dx \, \rho_{ha} \, L_v(w - w_w) \tag{10}$$

where h_c is the convective heat transfer coefficient.

Equation (10) can also be expressed as

$$\frac{d\dot{q}}{dx} = h_c \, p \left[(T - T_w) + \frac{Sh}{Nu \, Le} \frac{L_v}{c_{P,ha}} (w - w_w) \right] \tag{11}$$

where $Sh = h_D \, D/D_v$ is the Sherwood number, D_v is the vapor diffusivity coefficient, $Nu = h_c \, D/k_{ha}$ is the Nusselt number, $Le = k_{ha}/(\rho_{ha} \, c_{P,ha} \, D_v)$ is the Lewis number, and $c_{P,ha} = c_{P,a} + w \, c_{P,v}$ is the humid air specific heat. In configurations such like ours, the ratio $Sh/(Nu \, Le)$ is considered to be close to 1. Therefore, the energy conservation writes

$$\frac{d}{dx} h_{ha} = \frac{h_c \, p}{\dot{m}_a \, c_{P,ha}} \Big[c_{P,ha}(T - T_w) + L_v[w - w_w] \Big] \tag{12}$$

or

$$\frac{d}{dx} h_{ha}(T, w) = \frac{h_c \, p}{\dot{m}_a \, c_{P,ha}} [h_{ha}(T_w, w_w) - h_{ha}(T, w)] \tag{13}$$

Considering that at the pipe inlet (x = 0) $h = h_{in}$, we have

$$\bar{h} = \frac{h - h_w}{h_{in} - h_w} = exp\left(- \frac{h_c \, p}{\dot{m}_a \, c_{P,ha}} x \right) \tag{14}$$

where for the sake of clarity we wrote $h_{ha}(T, w) = h$, and $h_{ha}(T_w, w_w) = h_w$.

Note that this approach is still valid if T_w exceeds T_{in}, meaning that it is suitable if the EAHE is used for pre-heating instead of pre-cooling.

3.2 Case studies

As an application, we consider now two case studies: The inlet conditions, representative of a tropical climate (hot and humid), are $T_{in} = 27°C$ and $RH_{in} = 85\%$, while they are $T_{in} = 27°C$ and $RH_{in} = 62\%$ to be close to a continental climate in summer (hot and dry). In the latter, the ground temperature is 19°C. A ground temperature of 23°C was picked in the first case, both corresponding to a depth of almost 3 m underground (see Fig. 3) and equal to T_w. In accord with Fig. 1, these two cases belong to configuration A. Under the drier climate, the wall temperature is nearing the dew point temperature, while the difference between the two temperatures is more significant for the hot and humid conditions.

13

Note that the objective here is not to model actual underground networks but rather to compare the merit of the EAHE in two very different climatic conditions. To this sake, the pipe diameter was fixed to D = 10 cm and the mass flow rate was chosen to be $\dot{m} = 40$ g/s. Keeping these values in mind, it is now possible to check the assumption that led to Eq. (10). In the case of a duct with a uniform wall temperature in turbulent flow, the Nusselt number is given by the Dittus and Boelter correlation [29]

$$Nu_D = 0.023\, Re_D^{4/5}\, Pr^{1/3} \tag{15}$$

Here $Nu_D \cong 68.3$, and $Re_D \cong 23\,000$.

By the same token, the Sherwood number can be obtained by substituting the Prandtl number by the Schmidt number ($Sc = \nu/D_v \cong 0.63$)

$$Sh_D = 0.023\, Re_D^{4/5}\, Sc^{1/3} \tag{16}$$

Here $Sh_D \cong 60$. Because the Lewis number (Sc/Pr) is 0.88, the ratio $Sh/(Nu\, Le)$ is indeed about 1.

The analytical approach proposed so far assumes that the entire wall surface is wet. This is an extreme case, the opposite one being that the duct surface remains dry (i.e. moisture condensation or evaporation is not accounted for). Hence, the total enthalpy corresponding to such case is calculated by maintaining the latent contribution equal to the inlet condition, which is equivalent to a more classical approach where heat transfer only is considered. We present in Fig. 6 the evolution of the total enthalpy along the duct in those two cases as a function of the pipe length in the hot and dry climate (in summer). h_1 is the total specific enthalpy accounting for both sensible and latent heat transfers, while h_2 represents the total specific enthalpy when only sensible exchanges are considered

($w = w_{in}$). The results are given in the non-dimensional form defined in Eq. (14). In this case, the latent heat exchanges are not significant as the 2 curves are almost superimposed.

Figure 7 shows the results for the humid climatic conditions. The latent heat exchange represents an important share of the total heat exchange because the difference between the dew point temperature and the wall temperature is higher. This is important because in most analysis of such EAHE, only the sensible heat exchanges are accounted for, which may lead to the erroneous conclusion that the implementation of the underground network is not worthy because of the low temperature decrease. Cooling potential is not only about temperature decrease but also moisture content reduction. Figure 7 shows that in reality the underground heat exchanger can lower the water content of the air blown at the exit of the pipe. As already mentioned in the introduction, this would not only lead to energy savings, but also improve indoor thermal comfort and reduce the risk of mold development indoor. Finally, Figs. 6 and 7 allow also to estimate the pipe length above which the total enthalpy remains constant. According to the methodology presented here, this length is between 50 and 60m.

4. Time-dependent problem

First, we present a 3D model accounting for conduction heat transfer in the soil and combined to the latent and sensible heat exchanges along the pipe. The results obtained with the 3D model are compared to the results of the unsteady-state version of the model developed in Section 3.1. In the former the wall temperature is calculated from the heat exchanges between the soil and the air flowing along the pipe, in the latter T_w is given by Eq. (1) at the depth where the pipe is buried.

4.1 EAHE performances assessment including heat transfer in the soil

We consider a 3D model for the unsteady heat conduction in the soil, combined with a 1D model for the pipe with an approach equivalent to what was developed in steady state. The soil volume is parallelepiped of length L (variable), height H, and width W. We chose H = 15m, W = 5m [10]. The

15

soil thermal diffusivity is identical to the one previously chosen. The pipe of length L (obtained from Section 3.2) is positioned at a depth of 3 m from the soil surface (see Fig. 8).

Fourier's law of conduction is solved in 3D and non steady state for the soil, while the presence of the underground pipe acts as a heat source (or sink) to the ground. The heat emitted by the source (or received by the sink) is calculated per unit length of pipe, once the energy balance is solved along the pipe, keeping in mind that the ratio $Sh/(Nu\,Le)$ is about 1. The wall temperature needed to determine the wall enthalpy is calculated from the energy balance at the wall, stating that the heat transfer from the soil is identical to the heat flux inside the pipe.

The energy balance which was defined initially in steady state in Eq. (13), becomes

$$\rho_{ha}A\frac{dh}{dt} = -\dot{m}_a\frac{dh}{dx} + \frac{h_c\,p}{c_{P,ha}}[h_w - h] \tag{17}$$

which means that in this case, the duct wall is assumed to be wet all along. Here, A is the pipe cross section. The pipe perimeter which appears in Eq. (17) is the same as in the steady state configuration (diameter of 10 cm). The mass flow rate is kept at 40 g/s. Equation (17) was implemented in the PDE (partial differential equations) module of a finite elements numerical code [30].

The boundary conditions are given by Eq. (1) at the soil surface (z = 0). A symmetry condition is imposed on all the other faces of the soil volume. The air temperature and relative humidity are provided at the entrance of the pipe from the weather data (Rio do Janeiro or Montpellier). A zero enthalpy flux condition is chosen at the exit of the pipe. The initial temperature condition for the entire domain is T_m from Table 1, and the initial moisture content is determined at the same temperature for a relative humidity of 100%. Mesh refinements were performed to make sure that the results do not depend on the elements number and size. Table 2 gives an example of the tests.

Table 2: Mesh test

Montpellier, L=50m, simulation period: January					
1D model			3D model		
Number of elements	$h_1(L)$, kJ/kg	Relative difference	Number of elements	$h_1(L)$), kJ/kg	Relative difference
50	39.58707773	2.24866E-07	298	40.86701648	0.003005702
100	39.58708663	0	490	40.74418239	0.00090529
500	39.58708663		1257	40.70729709	
Rio de Janeiro, L=60m, simulation period: January					
1D model			3D model		
Number of elements	$h_1(L)$), kJ/kg	Relative difference	Number of elements	$h_1(L)$), kJ/kg	Relative difference
50	70.39640896	0	289	68.73681939	0.000599529
100	70.39640896	5.5E-08	574	68.69560965	8E-05
500	70.39641283		1310	68.69011405	

We show in Figs 9 and 10 the results obtained respectively for the case in France (Montpellier) and in Brazil (Rio do Janeiro). Here L is 50 m for the French case, and 60 m in the case of Brazil. The results are given for one full year starting on January 1st, with a time step of 1 hour. Plotted in these two figures are the differences between the total enthalpies at the duct outlet and inlet, considering both sensible and latent heat transfers (h_1) if the pipe wall is wet all along.

Plotted also in Figs. 9 and 10 is the relative error made in solving the problem with the 1D model. In this case, we solved Eq. (17) alone with the same initial conditions in the pipe and the same inlet and outlet boundary conditions. Eq. (1) was applied to calculate T_w at z = 3m. Table 3 shows the corresponding mean error and the standard deviation

Table 3: 1D model

	Mean Error (kJ/kg)	Standard deviation (kJ/kg)
Montpellier	0.13	1.91
Rio do Janeiro	3.78	4.55

In sum, the 1D approach follows with a reasonable accuracy the enthalpies evolutions in time predicted by the 3D approach.

Figure 11 shows the evolution of the soil temperature over 1 year at different depths in the case of Montpellier and Rio do Janeiro. The values were recorder at the abscissa x = L/2. Remember that the pipe depth is 3m in this example. At t = 0, the soil temperature is a constant, while the temperature surface is given by Eq. (1). At a depth of 3m the soil temperature follows the general trend exhibit by the other temperature profiles, yet in a much less smooth way due to the interactions with the pipe. Plotted in Fig. 12 is the evolution of the heat transfer with the soil along the pipe line during one full year. The figure at the top corresponds to Montpellier, the one in the bottom shows the results for Rio do Janeiro. The calculations are all based on the actual weather data. The trends shown in Fig. 12 indicate that, based on the assumptions of the study, there is no impact in time of the presence of the pipe.

4.2 EAHE performances by using an analytical model for the wall temperature

The 1D approach is pursued to assess the cooling/heating potential of different regions in Brazil. Note that this approach is complementary to the one proposed in Section 2 and plotted in Fig. 4, considering the enthalpy instead of the temperature. It gives information not only on the period when the EAHE is relevant for cooling but also on the heat transfer intensity. Moreover the influence of the pipe length can easily be studied.

The 1D model was run with several tube lengths: L= 20m, and 30m, together with the length obtained from the steady state analysis (50m). Plotted in Figs. 13 and 14 are the enthalpy changes over the course of 1 year when sensible and latent heat exchanges are considered (h_1), and when only the sensible enthalpy exchange is accounted for, the latent enthalpy being kept at its entrance value (h_2). The climate of Rio was selected as an intermediate behavior compared to the other Brazilian climates (Fig. 4). The values presented in Figs. 13 and 14 are the inlet and outlet enthalpies, together with the wall enthalpy, which is considered constant along the pipe. Recall that this means that at

every time step the moisture content is $w(L)$ to calculate $h_1(L)$ whereas it is w_{in} for $h_2(L)$. From the $h_1(L)$ curves we can see the effect of the tube length on the outlet total enthalpies: they become controlled by the wall conditions when the pipe length approaches the value obtained with the steady-state assumption. This latest result shows that the steady-state approach is relevant for determining the maximal length of the EAHE. Figures 13 and 14 represent actually the envelope between the two extreme cases.

To ease the analysis of the results presented in Figs. 13 and 14, the potential of heating and cooling was determined by plotting the monthly average difference between the enthalpy at the heat exchanger outlet and its inlet. Plotted are the total enthalpy differences together with the sensible ones. Figures 15 and 16 correspond respectively to Montpellier and Rio do Janeiro.

During the fall and winter in France (Figs. 13 and 15), the global trend of the enthalpy demonstrates the heating potential of the underground, as the enthalpy at the exit is higher than the one at the inlet. Moreover, a difference is noticed when latent heat transfer is accounted for, as the system can benefit from latent heat exchanges. From May to August, we see that that the results are very close on an average, meaning that the latent heat exchanges are not significant. Still, the ground cooling potential is clearly highlighted. The impact of latent exchanges is critical during the mid-season which corresponds to the months of April and September. Accounting only for sensible heat transfer, the air blown from the buried pipe would be considered as able to cool.

The trends exhibited in the case of Rio (Figs. 14 and 16) are drastically different. If the pipe is dry, the air at the exit of the duct has a specific enthalpy (h_2) lower than at the entrance during half of the year. It is the opposite when accounting for the latent heat exchanges along the pipe, except punctually in the very beginning of the Brazilian summer (November, see Fig. 14). The variability of the climatic conditions does not allow the soil to behave like an efficient heat exchanger. Sensible enthalpy can be decreased but the latent enthalpy is increased. Even though the EAHE can slightly impact the sensible enthalpy of the air blown into the building in the case of the tropical climate, Fig.

19

16 (Rio) shows that the latent enthalpy is always increased. The direct consequence is that the power of the air conditioning system needed in the building must be increased in order to dehumidify the indoor air, leading to the exact opposite expected result.

What should be the conditions for which an EAHE system meets the objectives of reducing the air conditioning needs under a climate such as the one of Brazil? Based on this idea, we looked for conditions that would correspond to the methodology proposed in Fig. 1. The region around Porto Alegre seems to be a good candidate. The mean annual temperature and relative humidity are 20°C and 74%, the annual temperature amplitude is 5K, as indicated in Table 1. The cooling and heating monthly potentials were plotted in Fig. 17. The results show that the EAHE allows to precool during summer (December and January) the blown air, even when accounting for the latent heat exchanges. Note that the decrease in enthalpy is lower for Montpellier (Fig. 15), yet the magnitude is of the same order.

5. Concluding remarks

Earth-Air heat exchangers are an old technique known since the Roman Empire around the Mediterranean Sea. Today, with the increasing concern in global warming and the objective of including renewable energy in the heating/cooling solutions for indoor comfort, EAHE experiences a renewed interest in several countries including Brazil. In this work we developed a model to account for latent and sensible heat exchanges between the buried pipe and the soil. By comparing the results to the climate of south of France, we look for the conditions when EAHE is an interesting solution. An example of tropical climate (Rio do Janeiro) was picked and the heat exchanges were envisaged in 2 extreme cases: considering sensible enthalpy only and adding latent heat exchanges when the pipe wall is wet. We show that the latent heat exchanges cancel the positive effect that the EAHE may have: Even though in summer the air is blown into the house at a lower temperature than the

20

outdoor; the air is humidified to such an extent that the air conditioning system would have to spend more power to maintain indoor comfort.

The 3D modelling of conduction heat transfer through the soil showed almost no difference with the approach consisting in calculating the pipe wall temperature at its buried depth from an analytical soil temperature function. The next step of this work will consist in including to the present study the hydric state of the soil and modelling its impact on the overall heat transfer through the pipe.

References

[1] Santamouris M, Mihalakakou G, Balaras CA, Argiriou A, Asimakopoulos D, Vallindras M. Use of buried pipes for energy conservation in cooling of agricultural greenhouses. Sol Energy 1995;55:111–24. doi:10.1016/0038-092X(95)00028-P.

[2] Santamouris M, Mihalakakou G, Balaras CA, Lewis JO, Vallindras M, Argiriou A. Energy conservation in greenhouses with buried pipes. Energy 1996;21:353–60. doi:10.1016/0360-5442(95)00121-2.

[3] Boulard T, Razafinjohany E, Baille A. Heat and water vapour transfer in a greenhouse with an underground heat storage system part I. Experimental results. Agric For Meteorol 1989;45:175–84. doi:10.1016/0168-1923(89)90042-7.

[4] Boulard T, Razafinjohany E, Baille A. Heat and water vapour transfer in a greenhouse with an underground heat storage system part II. Model. Agric For Meteorol 1989;45:185–94. doi:10.1016/0168-1923(89)90043-9.

[5] Kassem AS. Energy and water management in evaporitive cooling systems in Saudi Arabia. Resour Conserv Recycl 1994;12:135–46. doi:10.1016/0921-3449(94)90002-7.

[6] Al-Jamal K. Greenhouse cooling in hot countries. Energy 1994;19:1187–1192.

[7]   Hollmuller P, Lachal B. Air–soil heat exchangers for heating and cooling of buildings: Design guidelines, potentials and constraints, system integration and global energy balance. Appl Energy 2014;119:476–87. doi:10.1016/j.apenergy.2014.01.042.

[8]   Hollmuller P, Lachal B. Cooling and preheating with buried pipe systems: monitoring, simulation and economic aspects. Energy Build 2001;33:509–18. doi:10.1016/S0378-7788(00)00105-5.

[9]   Ascione F, Bellia L, Minichiello F. Earth-to-air heat exchangers for Italian climates. Renew Energy 2011;36:2177–88. doi:10.1016/j.renene.2011.01.013.

[10] Al-Ajmi F, Loveday DL, Hanby VI. The cooling potential of earth–air heat exchangers for domestic buildings in a desert climate. Build Environ 2006;41:235–44. doi:10.1016/j.buildenv.2005.01.027.

[11] Brum R da S, Vaz J, Rocha LAO, dos Santos ED, Isoldi LA. A new computational modeling to predict the behavior of Earth-Air Heat Exchangers. Energy Build 2013;64:395–402. doi:10.1016/j.enbuild.2013.05.032.

[12] Mihalakakou G, Santamouris M, Asimakopoulos D. Modelling the thermal performance of earth-to-air heat exchangers. Sol Energy 1994;53:301–5. doi:10.1016/0038-092X(94)90636-X.

[13] Vaz J, Sattler MA, dos Santos ED, Isoldi LA. Experimental and numerical analysis of an earth–air heat exchanger. Energy Build 2011;43:2476–82. doi:10.1016/j.enbuild.2011.06.003.

[14] Kim E-J, Roux J-J, Rusaouen G, Kuznik F. Numerical modelling of geothermal vertical heat exchangers for the short time analysis using the state model size reduction technique. Appl Therm Eng 2010;30:706–14. doi:10.1016/j.applthermaleng.2009.11.019.

[15] Pfafferott J. Evaluation of earth-to-air heat exchangers with a standardised method to calculate energy efficiency. Energy Build 2003;35:971–83. doi:10.1016/S0378-7788(03)00055-0.

[16] Serres L, Trombe A, Conilh JH. Study of coupled energy saving systems sensitivity factor analysis. Build Environ 1997;32:137–48. doi:10.1016/S0360-1323(96)00039-X.

[17] Paludetto D, Lorente S, Modeling the heat exchanges between a datacenter and neighboring buildings through an underground loop. Ren. Energy 2016;93:502-509. doi.org/10.1016/j.renene.2016.02.081

[18] Vaz J, Sattler MA, Brum R da S, dos Santos ED, Isoldi LA. An experimental study on the use of Earth-Air Heat Exchangers (EAHE). Energy Build 2014;72:122–31. doi:10.1016/j.enbuild.2013.12.009.

[19] Alves ABM, Schmid AL. Cooling and heating potential of underground soil according to depth and soil surface treatment in the Brazilian climatic regions. Energy Build 2015;90:41–50. doi:10.1016/j.enbuild.2014.12.025.

[20] Ozgener O, Ozgener L, Goswami DY. Experimental prediction of total thermal resistance of a closed loop EAHE for greenhouse cooling system. Int Commun Heat Mass Transf 2011;38:711–6. doi:10.1016/j.icheatmasstransfer.2011.03.009.

[21] Wolkoff P, Kjaergaard SK. The dichotomy of relative humidity on indoor air quality. Environ Int 2007;33:850–7. doi:10.1016/j.envint.2007.04.004.

[22] Soontornchainacksaeng T. Experimental and numerical study of the thermal behaviour of an Earth to Air heat exchanger designed for dwellings. INSA de Toulouse, 1993.

[23] Ozgener O, Ozgener L, Tester JW. A practical approach to predict soil temperature variations for geothermal (ground) heat exchangers applications. Int J Heat Mass Transf 2013;62:473–80. doi:10.1016/j.ijheatmasstransfer.2013.03.031.

[24] Hillel D. Introduction to soil physics. New York: Academic Press; 1982.

[25] Weather Data | EnergyPlus n.d. https://energyplus.net/weather (accessed May 27, 2016).

[26] :: INMET - Instituto Nacional de Meteorologia :: n.d. http://www.inmet.gov.br/portal/ (accessed August 10, 2016).

[27] Kepes Rodrigues M, da Silva Brum R, Vaz J, Oliveira Rocha LA, Domingues dos Santos E, Isoldi LA. Numerical investigation about the improvement of the thermal potential of an Earth-Air Heat Exchanger (EAHE) employing the Constructal Design method. Renew Energy 2015;80:538–51. doi:10.1016/j.renene.2015.02.041.

[28] Fan J, Ostergaard KT, Guyot A, Fujiwara S, Lockington DA. Estimating groundwater evapotranspiration by a subtropical pine plantation using diurnal water table fluctuations: Implications from night-time water use. J Hydrol 2016;542:679–85. doi:10.1016/j.jhydrol.2016.09.040.

[29] Dittus FW, Boelter LMK. Heat transfer in automobile radiators of the tubular type. Int Commun Heat Mass Transf 1985;12:3–22. doi:10.1016/0735-1933(85)90003-X.

[30] COMSOL Multiphysics. COMSOL Multiphysics Reference Manual. COMSOL®; 2014.

Figure captions

Figure 1   Identification of three areas in the psychrometric diagram for enthalpy variation in an EAHE for cooling.

Figure 2   Montpellier (France) and Brazil (the latter is from Ref. 12).

Figure 3   Minimum and maximum soil temperatures for Montpellier (France) and Rio do Janeiro (Brazil).

Figure 4   Estimation of η for Brazilian climates

Figure 5   EAHE system and model domain

Figure 6   Evolution of enthalpy in a continental climate zone.

Figure 7   Evolution of enthalpy in a tropical climate zone.

Figure 8   3D domain for the numerical simulations.

Figure 9   Difference between inlet and outlet enthalpies in the 3D case and in the 1D case, and relative error in the Montpellier (France) configuration.

Figure 10   Difference between inlet and outlet enthalpies in the 3D case and in the 1D case, and relative error in the Rio do Janeiro (Brazil) configuration.

Figure 11   Soil temperature variation over 1 year at different depth, x = L/2.

Figure 12   Heat transfer along the pipe line over 1 year.

Figure 13   Envelope of the enthalpy at the exit of the pipe, during one year in the case of Montpellier, France.

Figure 14   Envelope of the enthalpy at the exit of the pipe, during one year in the case of Rio do Janeiro, Brazil.

Figure 15   Cooling and heating potential in the case of Montpellier, France.

Figure 16   Cooling and heating potential in the case of Rio do Janeiro, Brazil.

Figure 17   Cooling and heating potential in the case of Porto Alegre, Brazil.

Figure 1

(a)
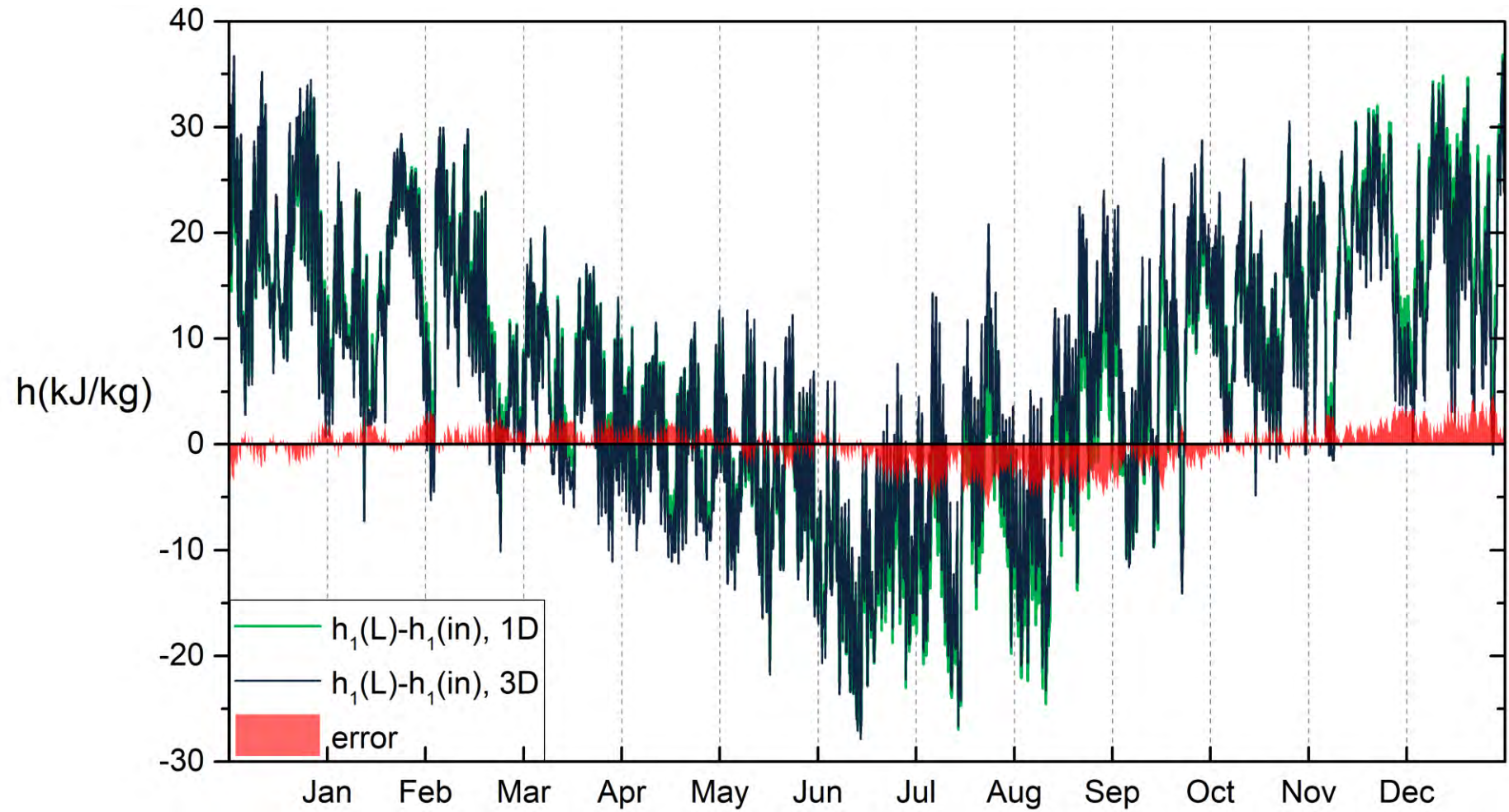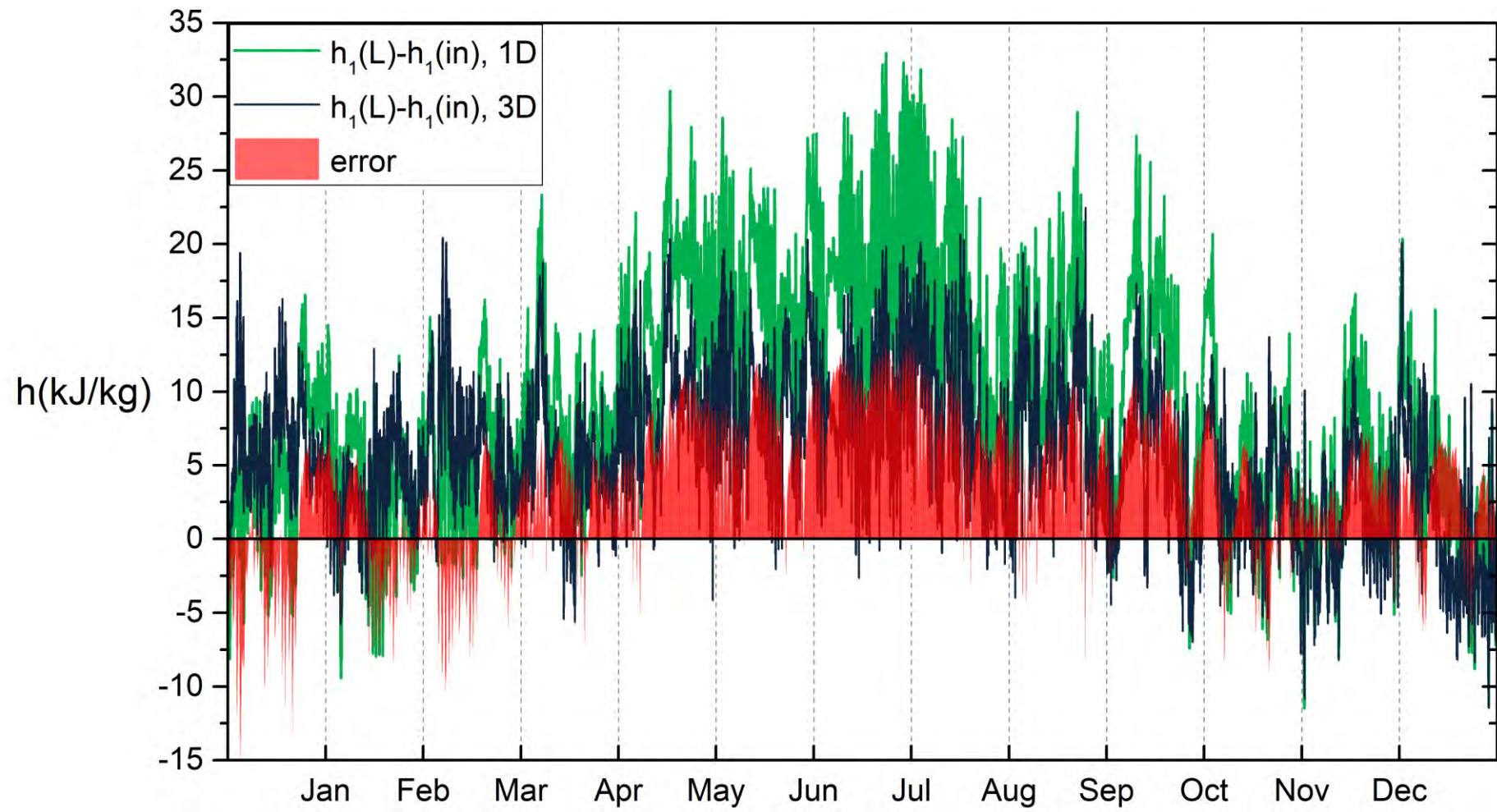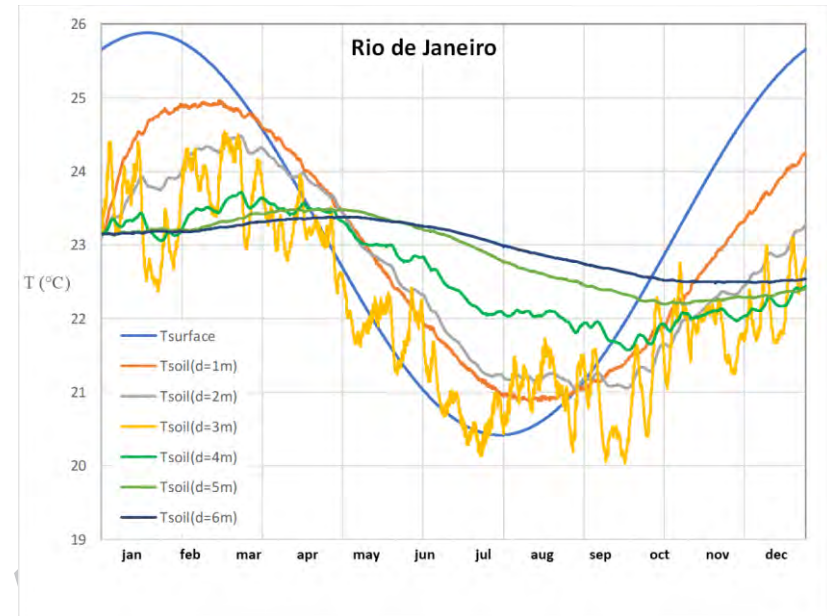
(b)
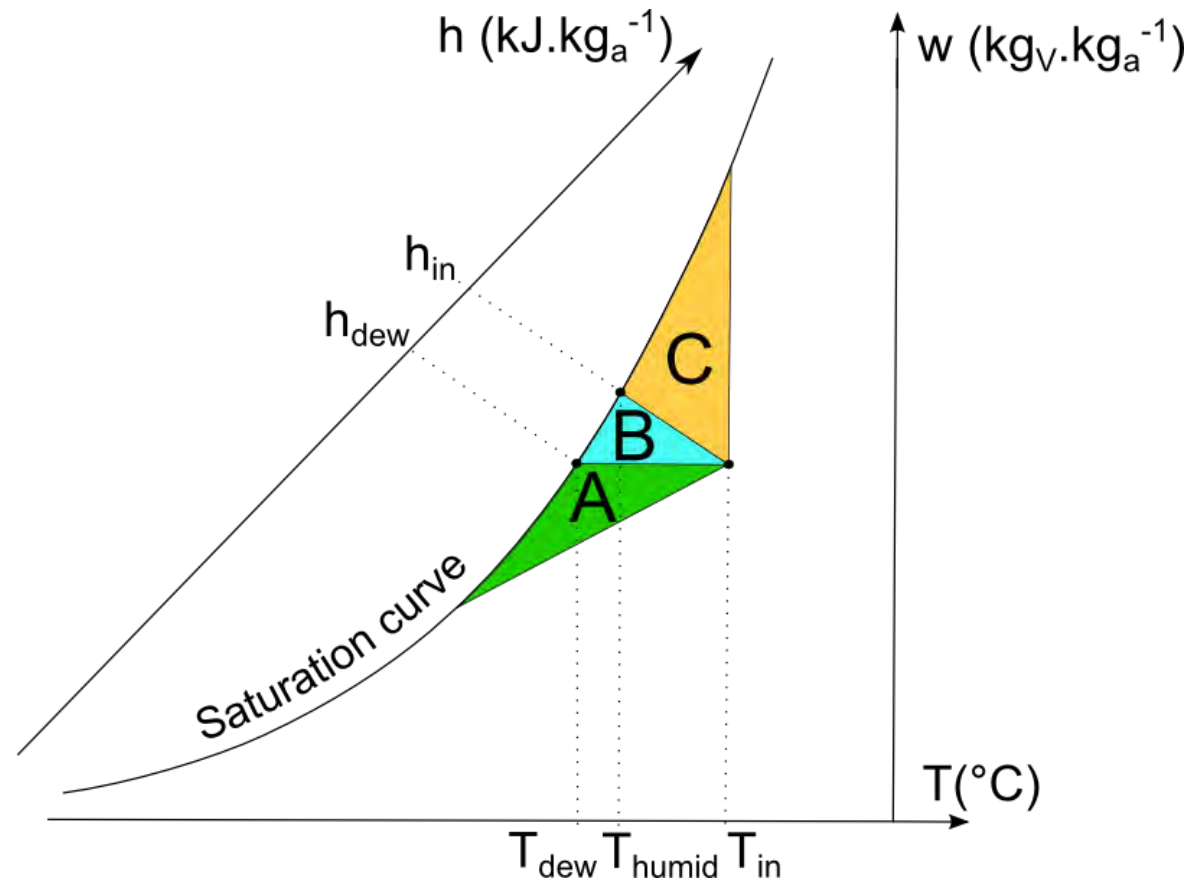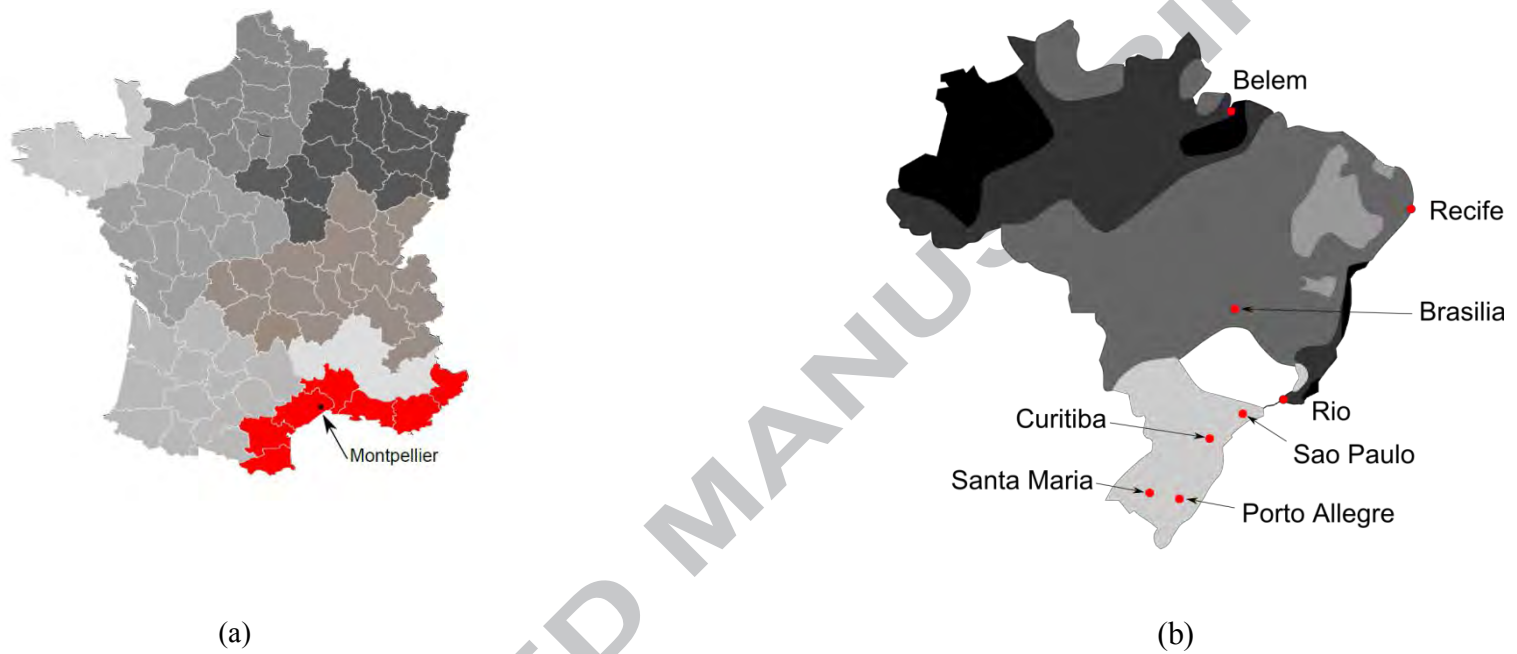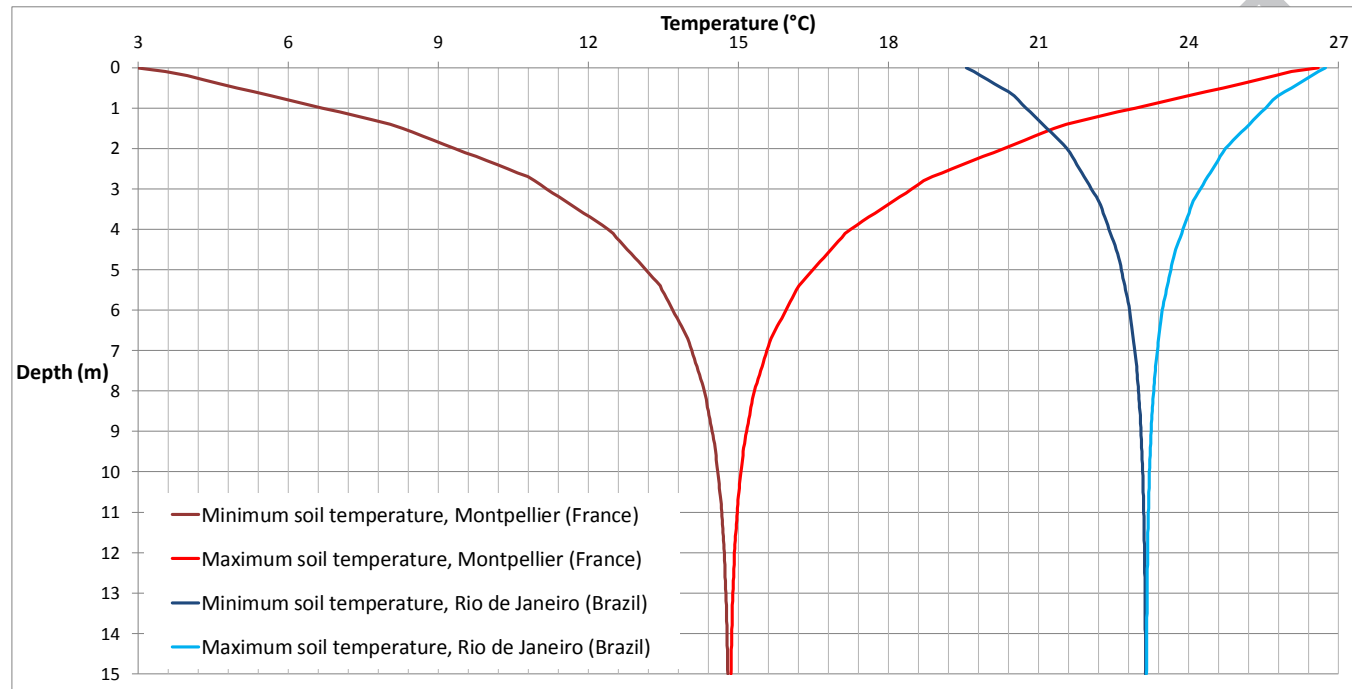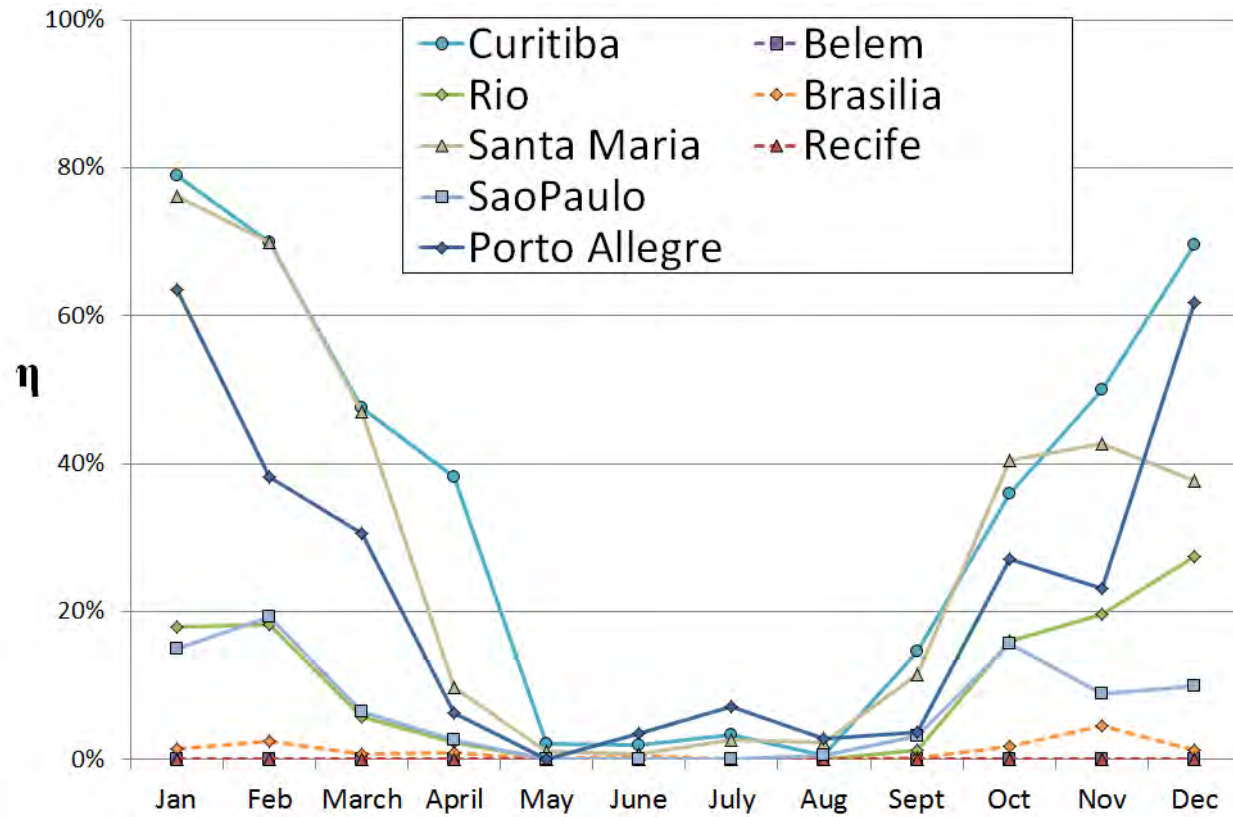
Figure 2

Figure 3

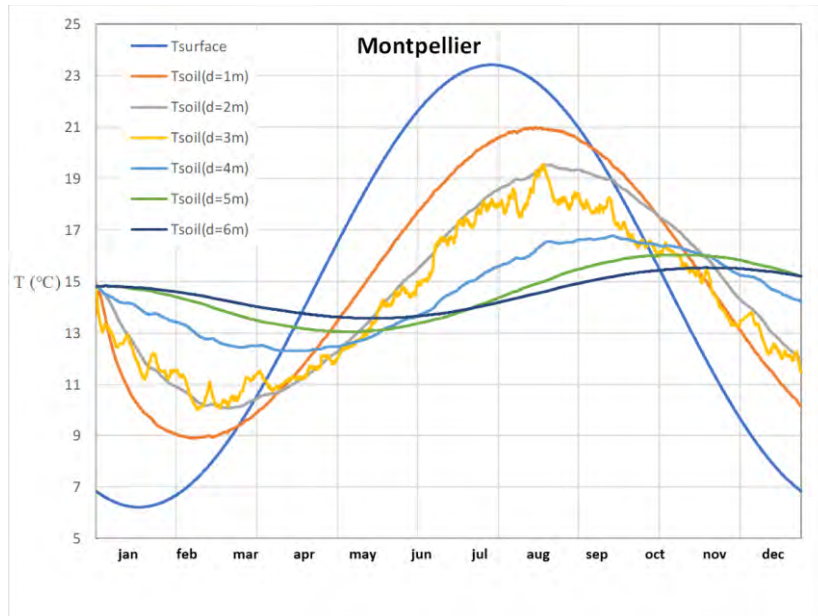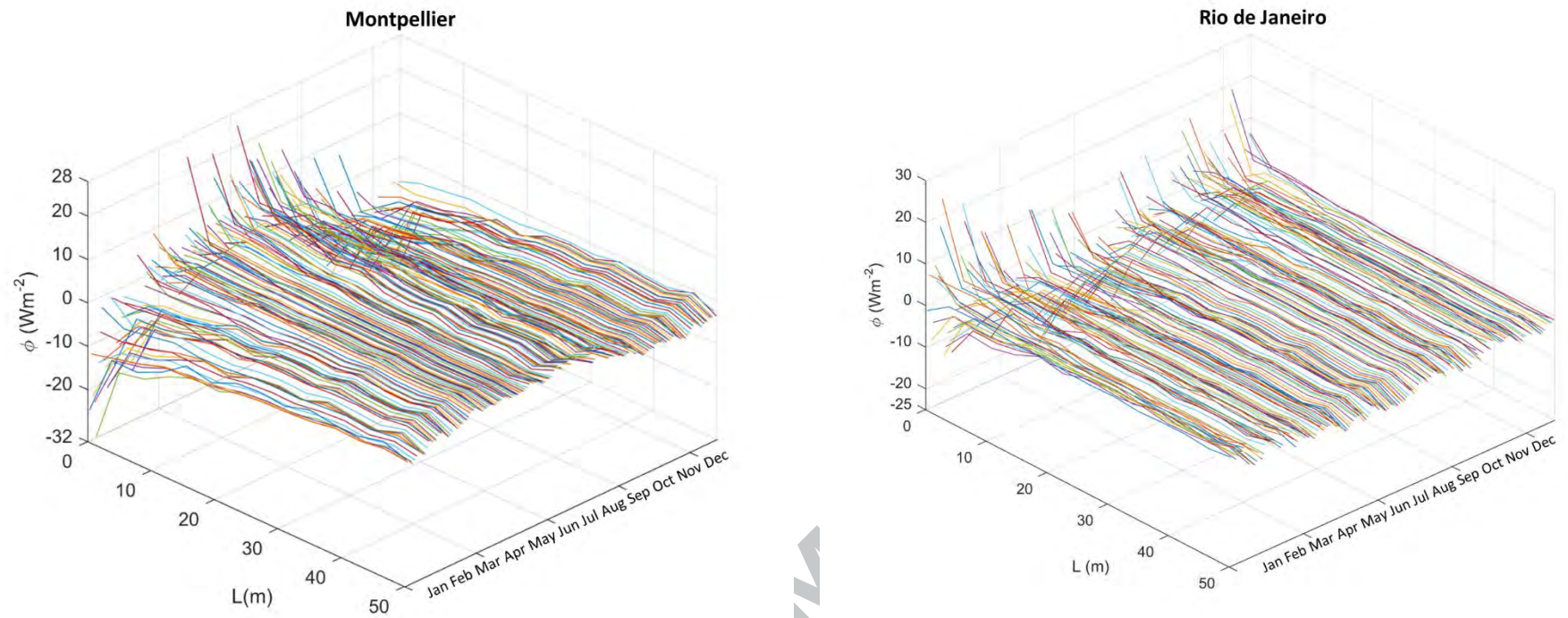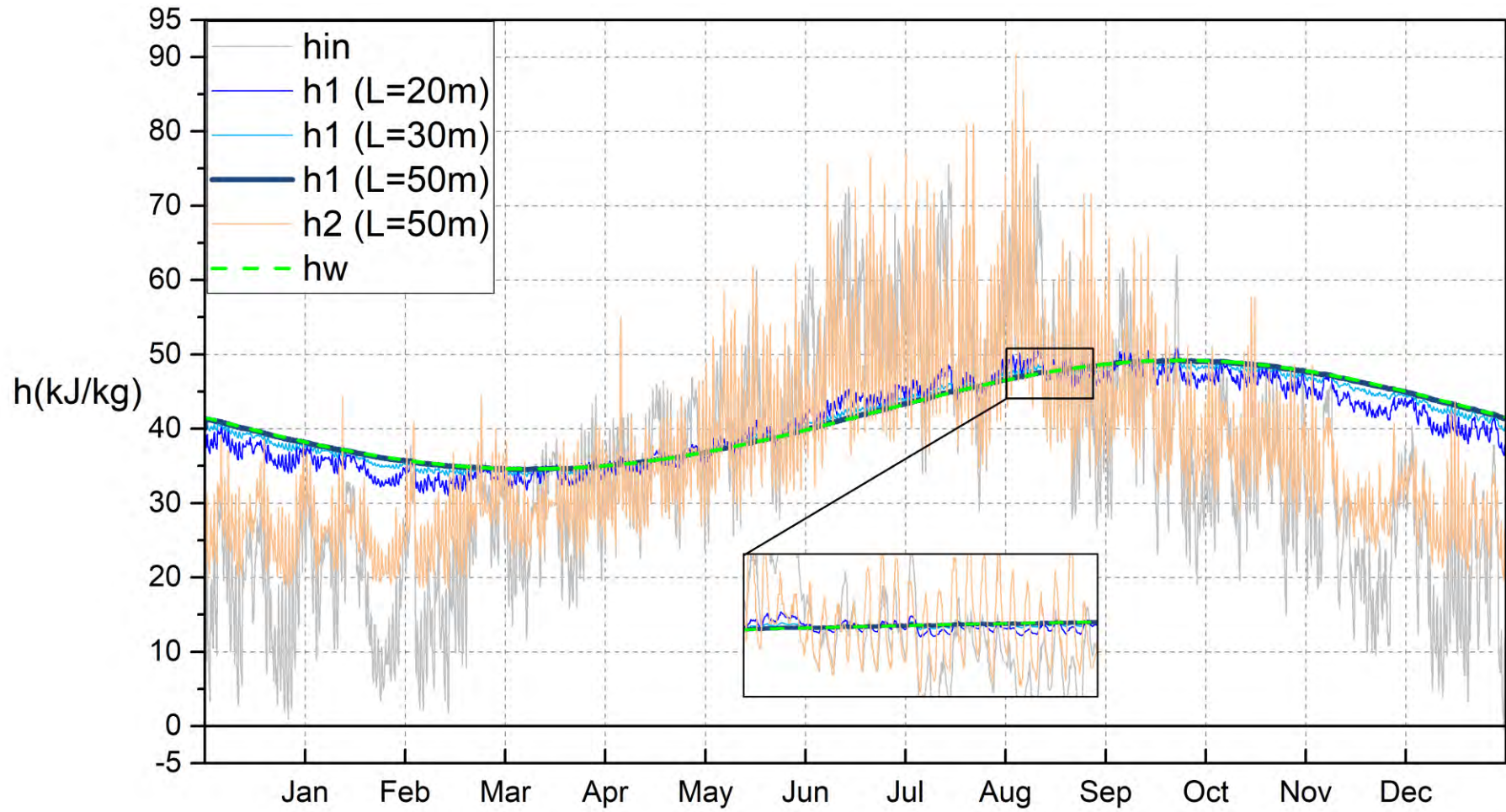Figure 4
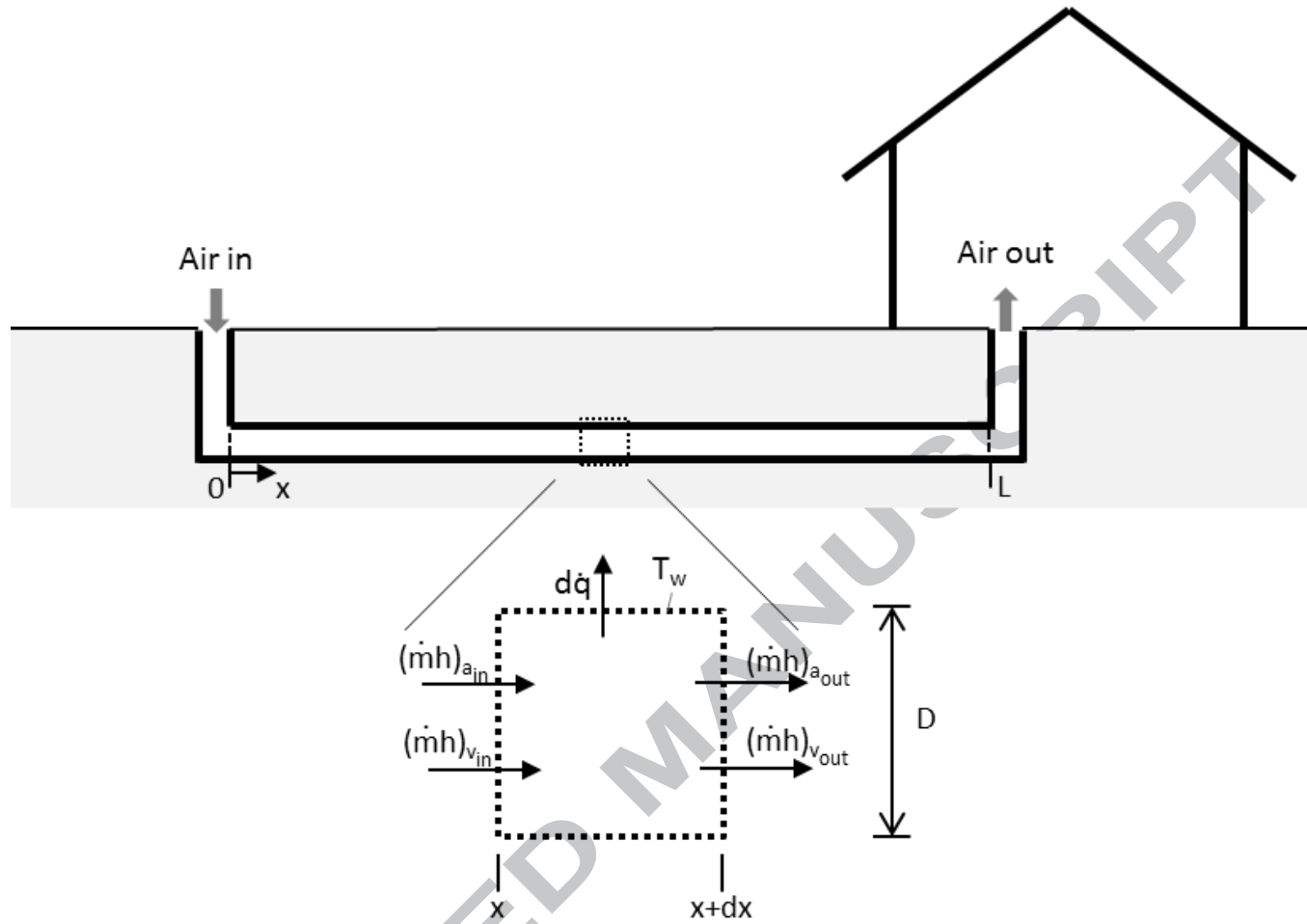
Figure 5
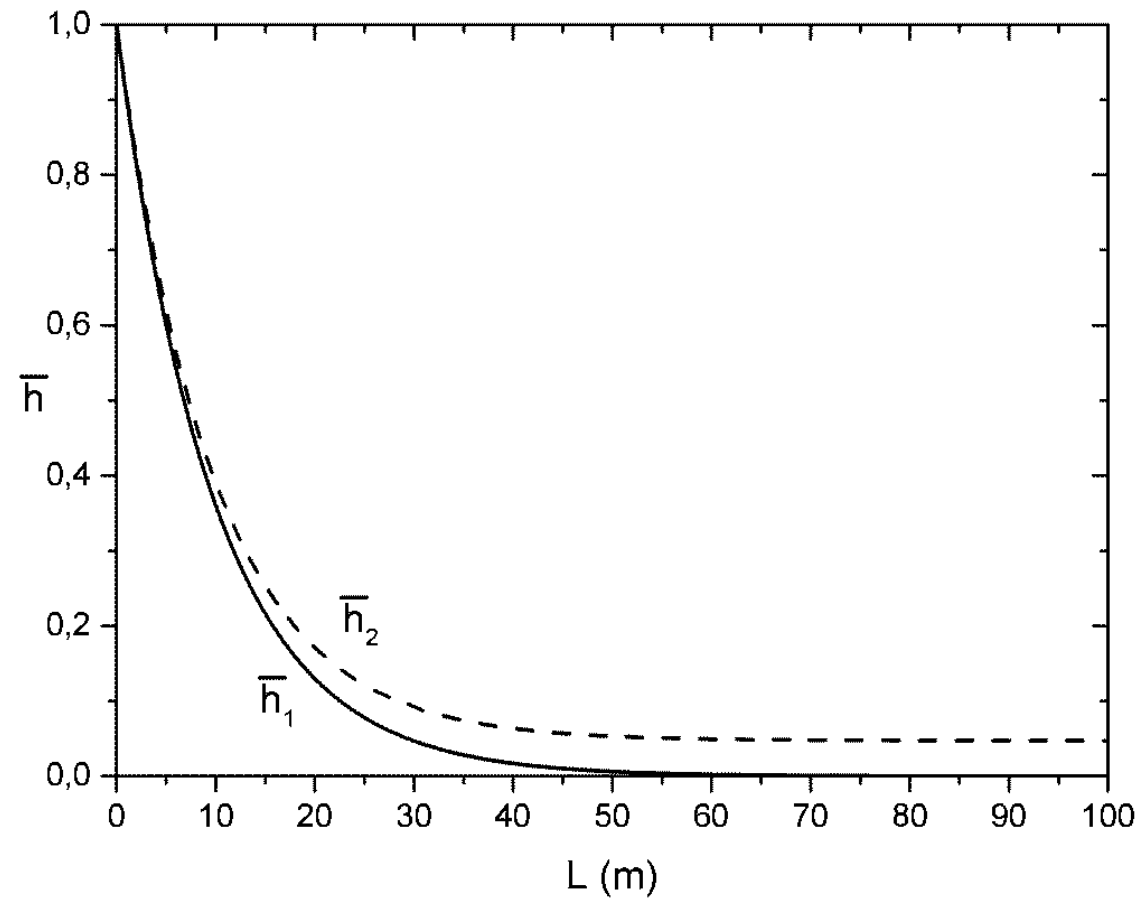
Figure 6
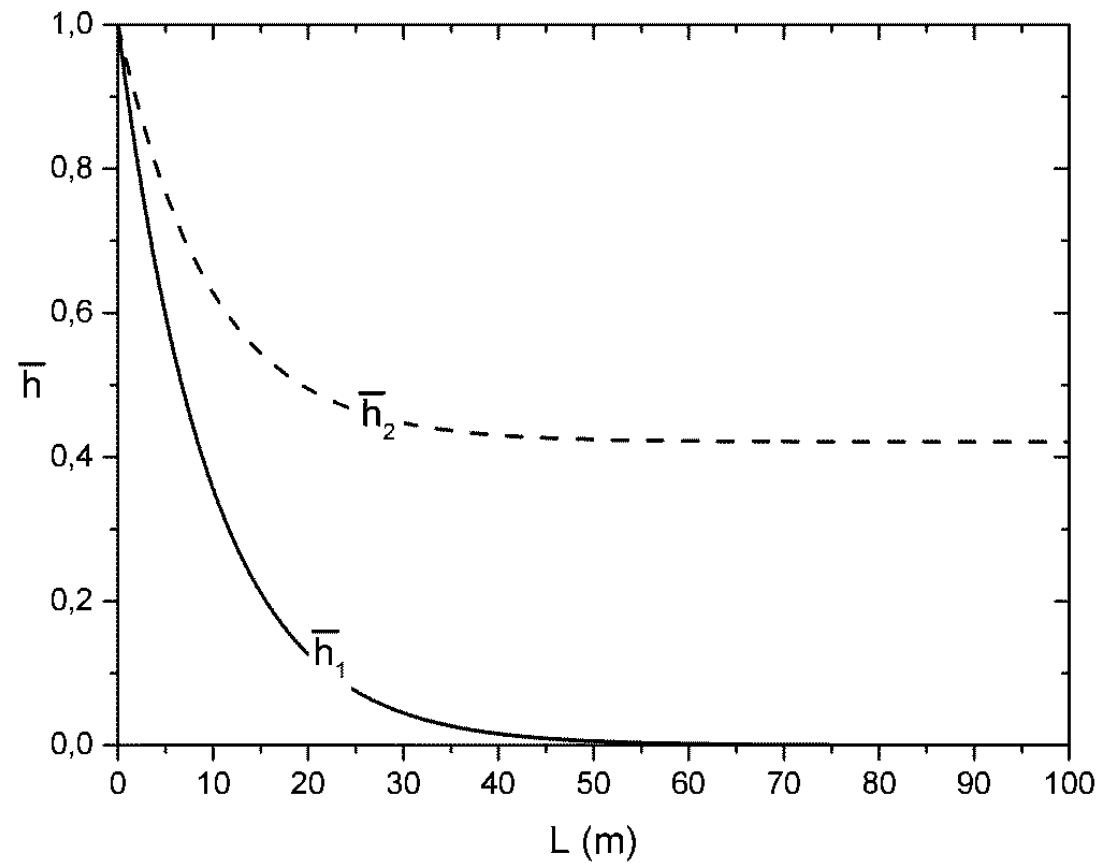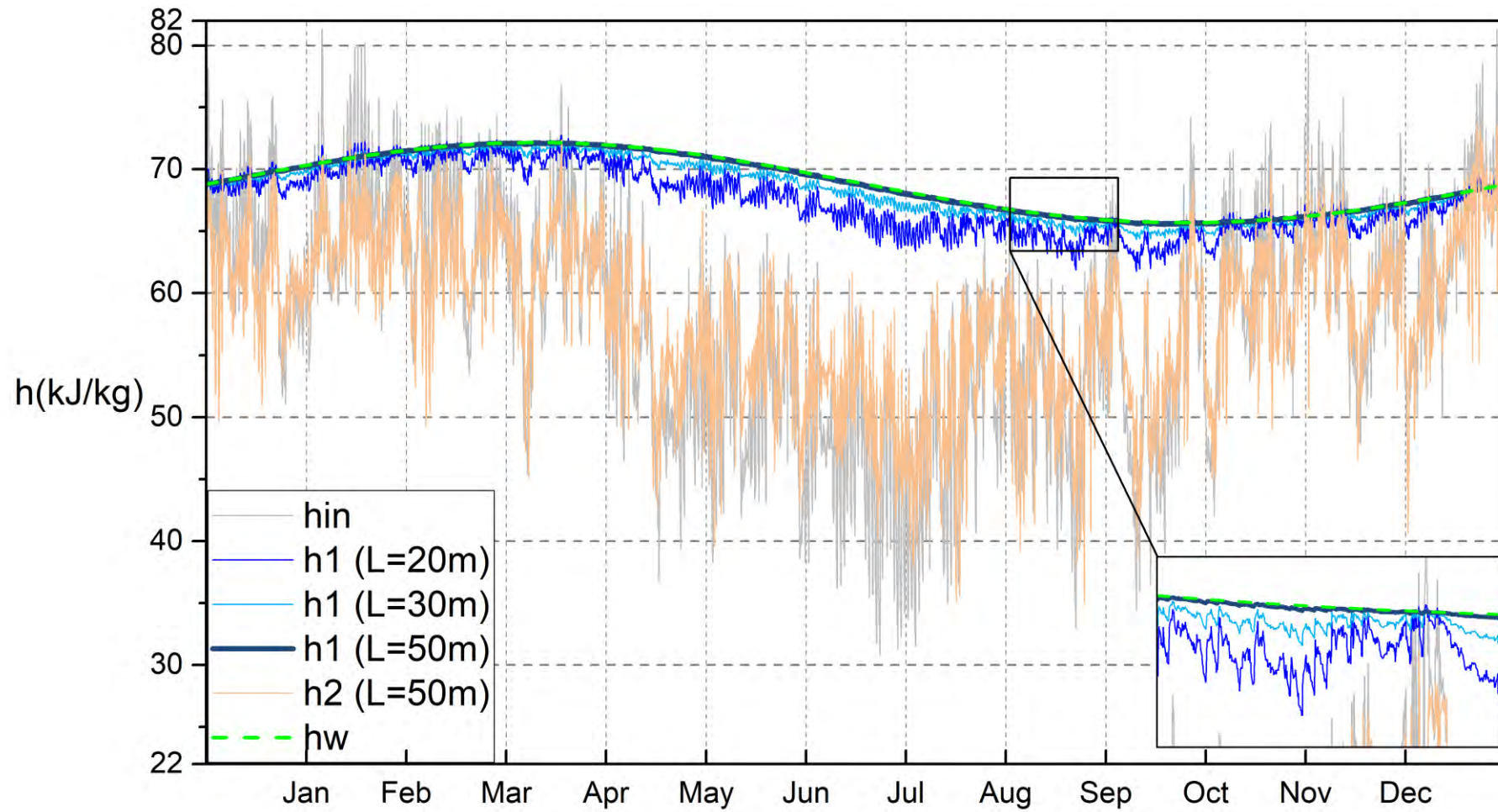
Figure 7

7
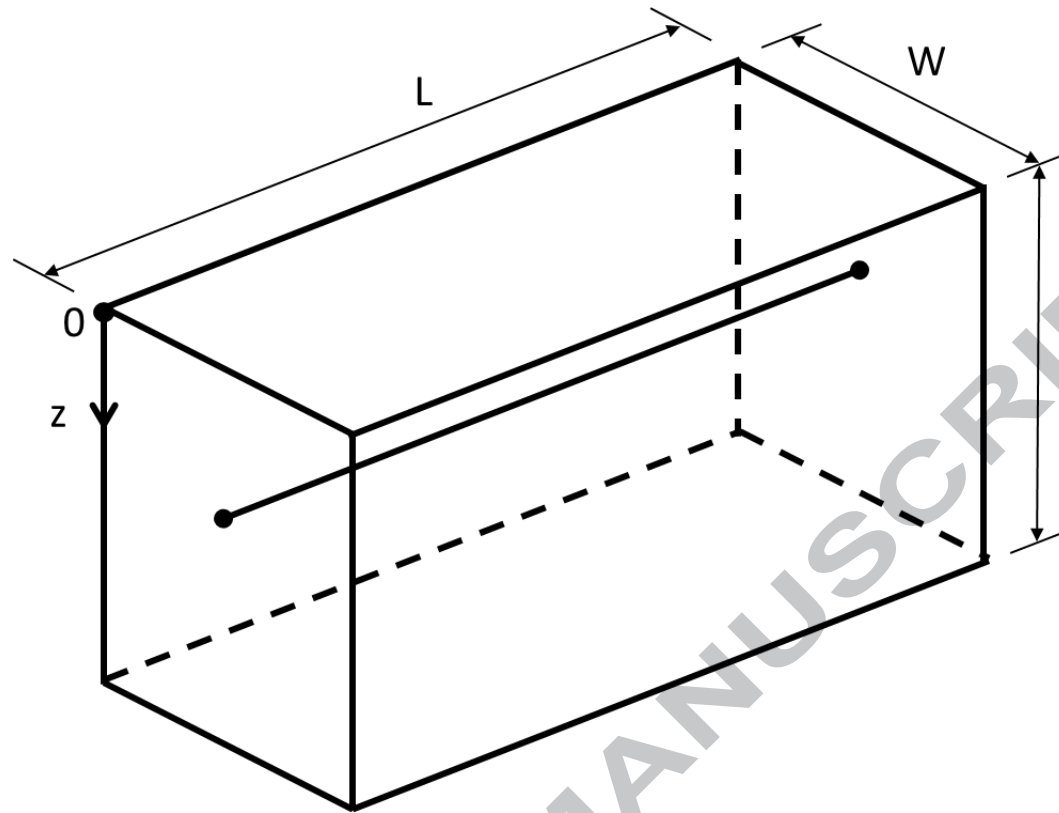
Figure 8

Figure 9
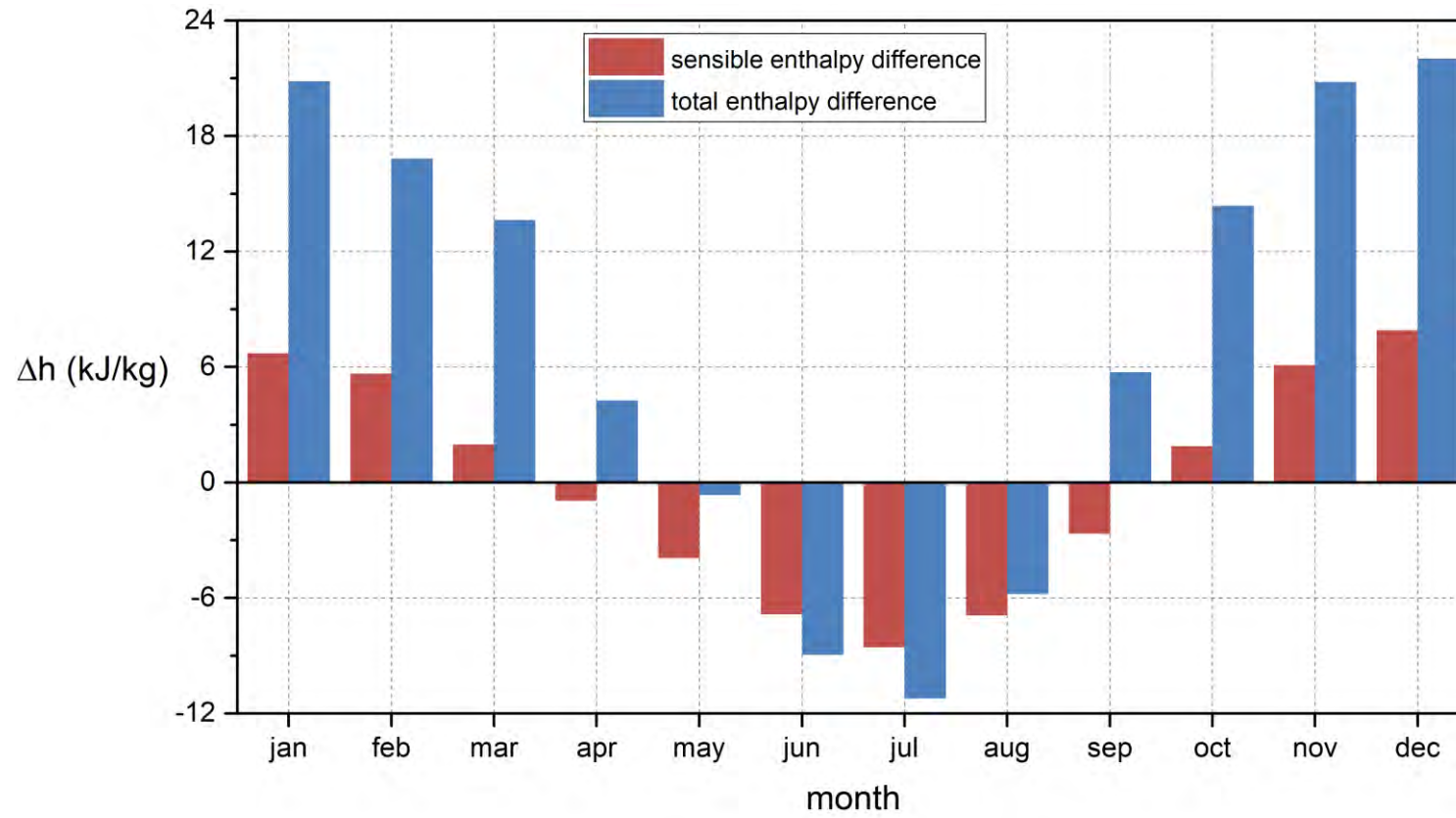
Figure 10
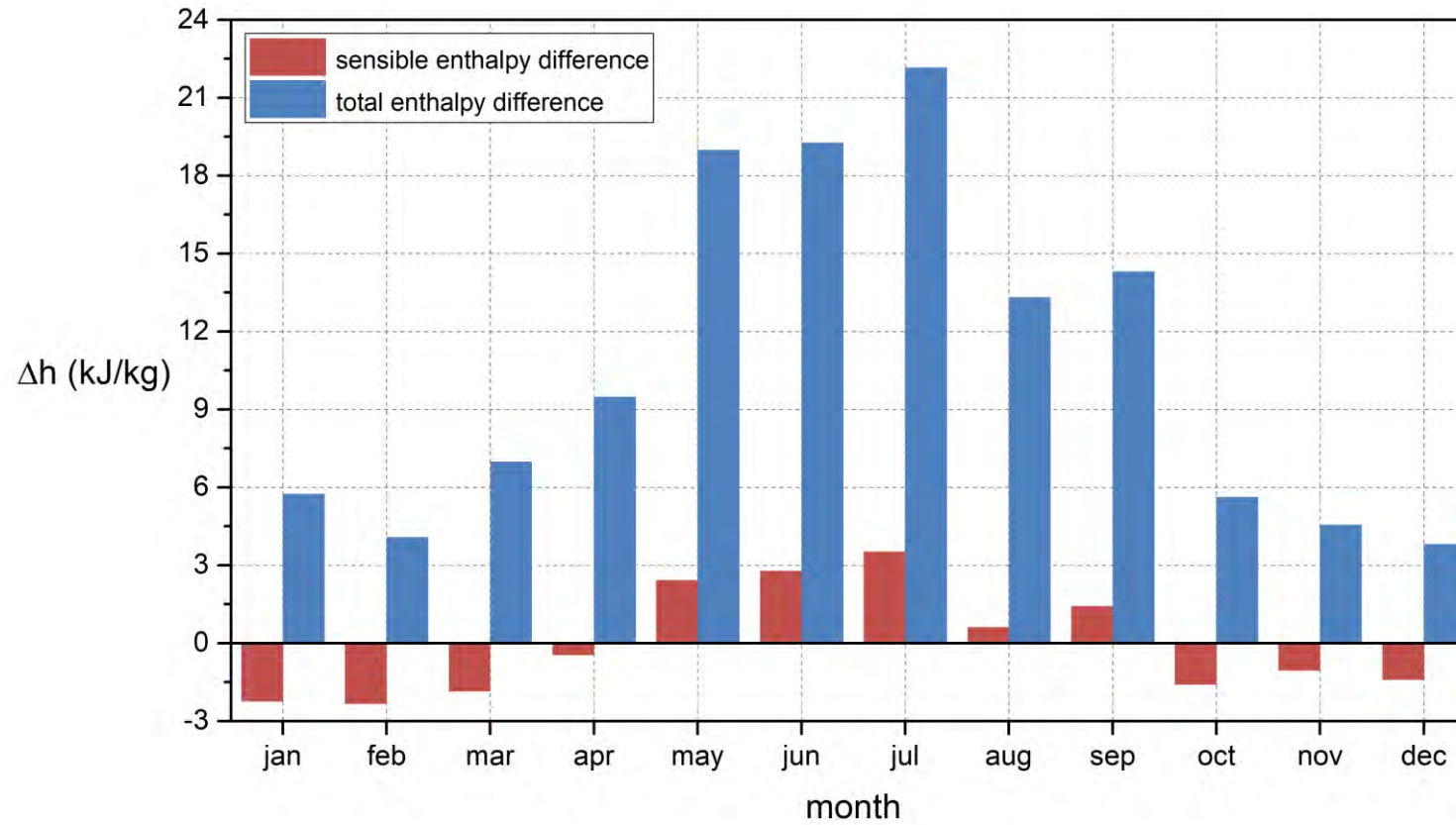
Figure 11
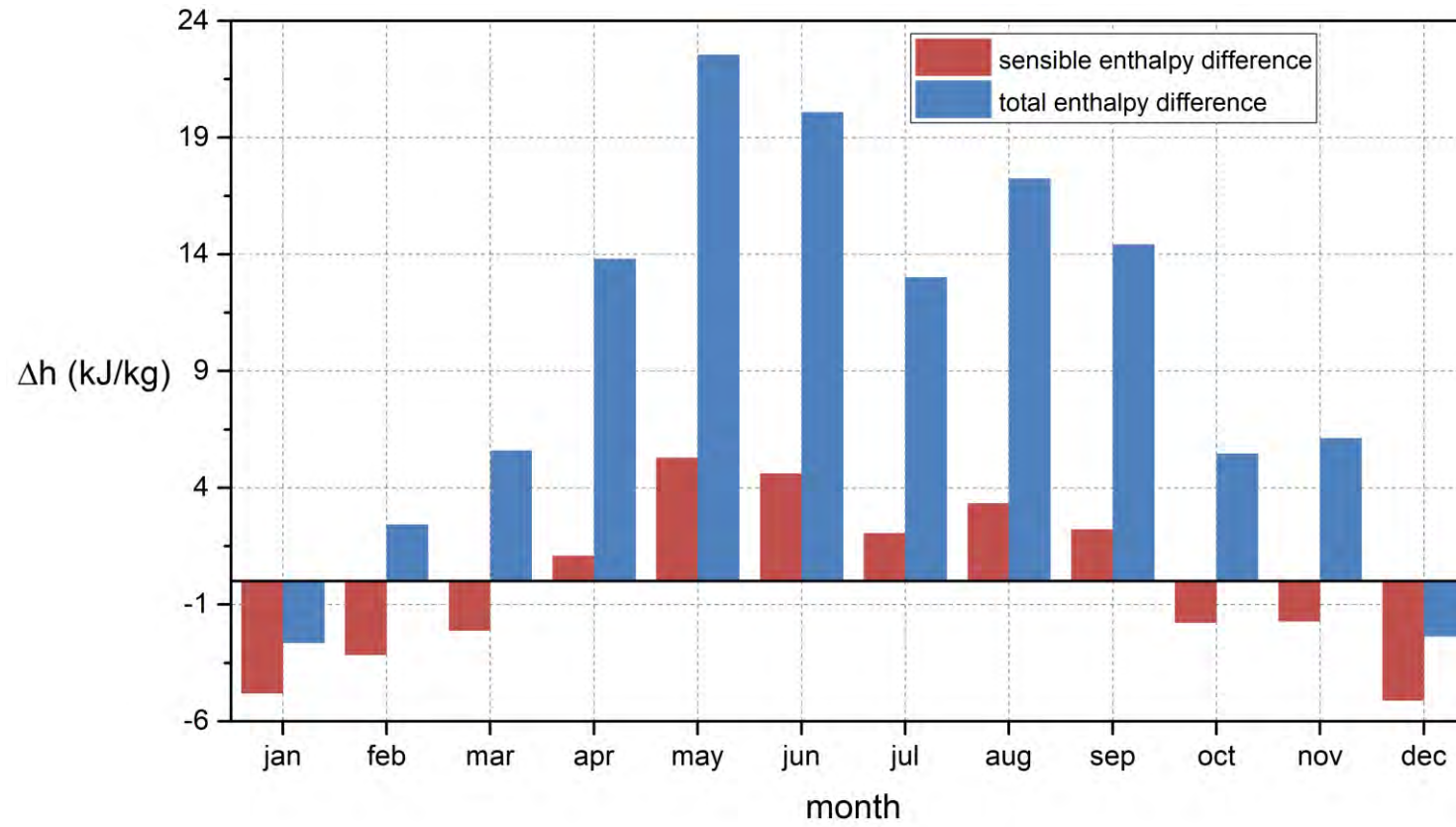
Figure 12

Figure 13

Figure 14

Figure 15

Figure 16

Figure 17

Highlights

Underground Earth Air Heat Exchangers (EAHE) in various climates are investigated.

A model describing EAHE sensible and latent heat exchanges is proposed.

Latent heat exchanges question the relevance and the positive effect of the EAHE.